MOISTURE DETECTION ABOVE CONVECTIVE STORMS UTILIZING THE METHOD OF BRIGHTNESS TEMPERATURE DIFFERENCES BETWEEN WATER VAPOR AND IR WINDOW BANDS, BASED ON 2008 MSG RAPID SCAN SERVICE DATA

Jindřich Šťástka[1,2], Martin Setvák[2], Michaela Radová[1,2,3], Daniel T. Lindsey[4], Alois Sokol[5]

[1]Charles University, Faculty of Mathematics and Physics, Department of Meteorology and Environment Protection, V Holešovičkách 2, CZ-18000 Praha 8, Czech Republic.
[2]Czech Hydrometeorological Institute, Na Šabatce 17, CZ-14306 Praha 4, Czech Republic.
[3]Institute of Atmospheric Physics, AS CR, Boční II 1401, CZ-14131 Praha 4, Czech Republic
[4]NOAA/NESDIS/RAMMB, CIRA/CSU, 1375 Campus Delivery, Ft. Collins, CO 80523, USA.
[5]Faculty of Mathematics, Physics and Inform., Comenius Univ., Mlynská dolina, Bratislava, Slovakia

Abstract

The BTD [WV-IRW] method based on the Brightness Temperature Difference (BTD) between WV and IR window bands has been used in previous studies to document the presence of water vapor above the tops of convective storms. This lower stratospheric moisture (LSM) can either be advected above the storms from remote locations, or injected into the lower stratosphere by the storm itself. Previous studies either addressed cases observed by polar orbiting satellites (thus being only "snapshots"), or presented individual cases documented by MSG/SEVIRI 15-minute data. The present study focuses on this topic using a large dataset of cases collected during the 2008 season, documenting the hypothesized above-storm-LSM by means of MSG Rapid Scan Service (RSS) 5-minute data, aiming primarily at storms over central Europe. Besides the detection and statistics of LSM based on this dataset, we will also try to determine if any particular storm type tends to generate enhanced LSM, including the life cycle of these storms, and at what time the storm becomes the most efficient at generating LSM.

INTRODUCTION

The transport mechanism of water vapor through the tropopause has been studied using numerical cloud models over the last several years (e.g. Wang et al, 2009). A better understanding of how tropospheric water can be injected into the lower stratosphere is essential for the estimation of the stratospheric WV budget. The amount of stratospheric water vapor is changing with time; some recent observations have shown that it has been increasing over the last few decades (Oltmans et al., 2000). The examination of issues such as LSM sources or its cross-tropopause transport mechanism is important because of their influence on global climate.

The main evidence of such a transport mechanism has been provided by satellite observations. The brightness temperature difference between water vapor absorption and infrared window bands is used for the detection of lower stratospheric moisture. Since the IR window band typically sees deeper into the warmer layers of the atmosphere than the WV band, the water vapor band radiance is usually lower than the IR window band radiance. The tropospheric moisture above lower cloud tops is usually colder than the cloud top brightness temperature, and since the WV band detects this colder water vapor, the BTD (defined as WV-IRW) is typically negative for most clouds and cloud-free areas. However, positive BTD values can be found above cloud tops of most convective storms. Fritz and Laszlo (1993) first noted that positive BTD values occur over storms in the tropics. Three years later, Ackerman (1996) discussed positive values in polar regions and Schmetz et al (1997) have documented positive BTD values even above the tops of deep convective storms in mid-latitudes. Satellite observations in those studies were limited by the imager's temporal and pixel resolutions. This paper benefits by using Meteosat Second Generation (MSG) Rapid Scan Service (RSS) data from the satellite's Spinning Enhanced Visible and Infrared Imager (SEVIRI). The bands used in this analysis were WV6.2 channel and the IR10.8 window channel.

WATER VAPOR EFFECTS ABOVE THETROPOPAUSE INVERSION

Different water vapor effects in the lower stratosphere, in the case of a temperature inversion above the tropopause, are illustrated in Figs. 1 - 4. The CloudSat profile from 26 January 2010 over Australia was used for these schematics, which are from Martin Setvák's presentation *Satellite observation of storm tops* presented at *EUMETSAT's Workshop on physics and dynamics of convective storms and their appearance in satellite imagery* in Prague in August 2010. Figure 1 shows a case with no moisture above the storm top. In this situation both bands detect radiation originating at the storm cloud top only. Thus, the brightness temperature (BT) in both of these bands is very similar, being affected by emissivity and transparency effects only. The BTD values are therefore close to zero for most of the storm top.

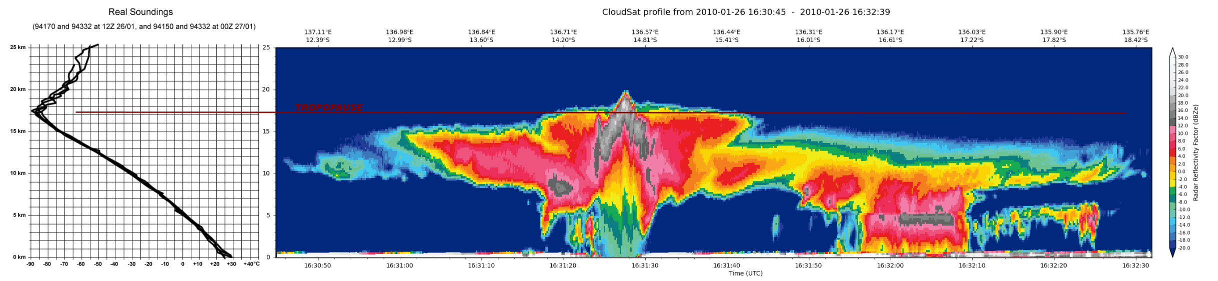

Figure 1: **Schematic with no moisture above the storm top – the CloudSat profile from 26 January 2010 over Australia (on the right) and several real nearby soundings from the closest term to the time when the storm occurred (on the left).**

The situation with a uniform layer of moisture above the tropopause is shown in Fig. 2. The warmer water vapor layer adds additional radiance in the WV band to the thermal emission originating from the cold storm top, but remains transparent to the IR window band. Therefore the brightness temperature is higher in the WV band as compared to the IR window band. The BTD values are thus positive above most of the storm top, closely correlated to the brightness temperature in the IR window band. Higher positive BTD values correspond to colder parts of the cloud-top. The highest positive BTD values are typically located above the overshooting tops, as these are usually the coldest parts of the storm top.

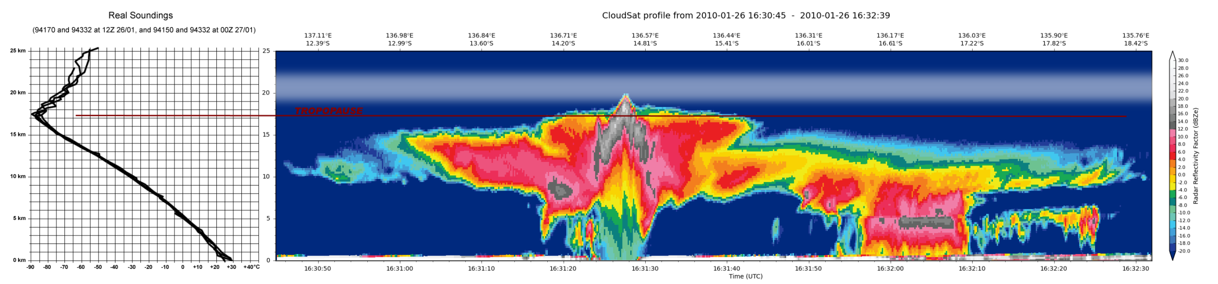

Figure 2: **The same schematic as in Fig. 1 but with a uniform layer of moisture above the storm top.**

If the moist layer is vertically thinner or lower, so that the highest overshooting tops can penetrate it, there is not enough warm moisture above them to increase the brightness temperature in the WV band (Fig. 3). In this situation we can still observe positive BTD above most of the storm top, closely correlated to the brightness temperature in the IR window band. However, the BTD values above the highest (coldest) overshooting tops are much lower, close to zero.

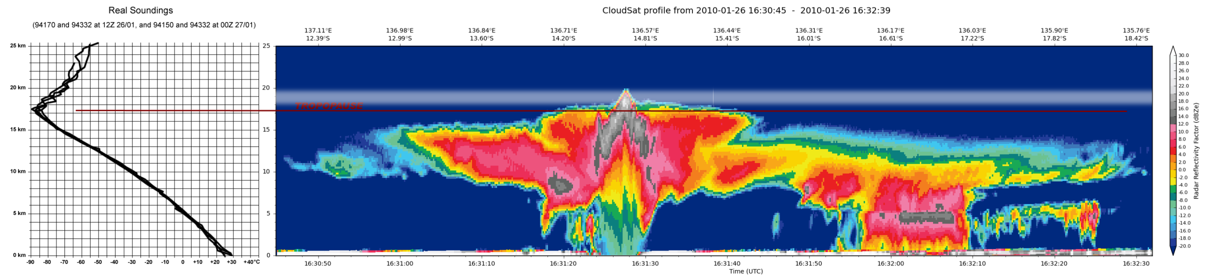

Figure 3: **The same schematic as in Fig. 1 but with a shallow (vertically thin) uniform layer of moisture at the storm top.**

The last schematic (Fig. 4) displays the case where the moisture is injected into the lower stratosphere locally by the storm itself. The brightness temperature in WV band can be increased only locally. The BTD values are positive above some parts of storm top only, not necessarily co-located with the coldest tops and thus not as correlated with the brightness temperature in the IR window band.

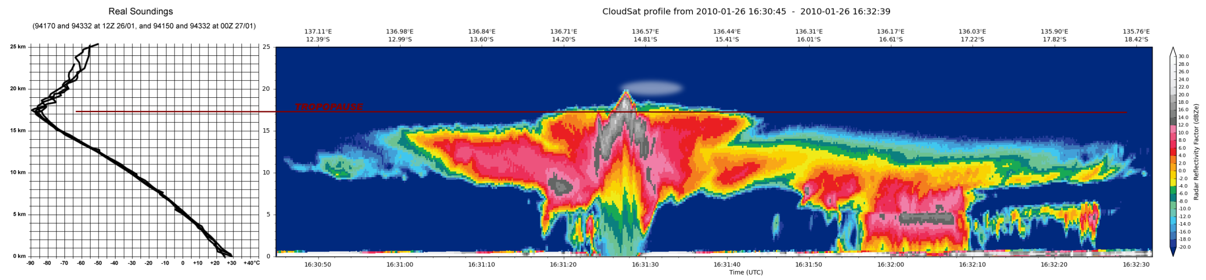

Figure 4: **The same schematic as in Fig. 1 but with locally generated moisture above the storm top.**

SATELLITE OBSERVATIONS

During the 2008 season we collected 33 cases (convective episodes). All of them were processed by VCS *2met!* Software for creating BTD data. The additional analysis was done by our own software written in IDL (Interactive Data Language).

In most cases the positive BTD values are closely spatially correlated to the brightness temperature field in IR window band, with the local BTD positive maxima co-located with the coldest pixels in the IR 10.8 band. This very likely indicates a uniform layer of warmer lower stratospheric moisture (LSM) above the storm tops. The LSM is not related to the storms themselves, but was probably advected from some other remote sources. This corresponds to the schematic shown in Fig. 2. An example of such a situation is the storm which formed near the border between Czech Republic and Poland on 15 August 2008 at about 1400 UTC. The convective system was active until about 0600 UTC the next day – 16 August 2008. Fig. 5 shows images from the most interesting parts of the storm evolution. The left column displays 10.8 µm images with color-enhanced brightness temperatures in the range 200 – 240 K; the middle panel depicts the BTD product with positive BTD values shown in a color scale from 0 K (dark violet) to 6 K (red) and negative values presented in grey shades; the right panel depicts scatterplots that present the relationship between 10.8 µm brightness temperature and BTD. As was already mentioned above, this case (Fig. 5) is an example of a close correlation between 10.8 µm and BTD fields, evident not only from MSG images but also from scatterplots. These demonstrate that pixels with higher positive BTD are associated with the lowest 10.8 µm brightness temperatures.

Fig. 6 shows the time evolution of mean BTD and mean 10.8 µm brightness temperature of all pixels having positive BTD values. The main increase of the mean BTD started at about 1845 UTC, as can be seen in Fig. 6 and also from a comparison of BTD images from 1800 UTC and 1845 UTC in Fig. 5. This increase of the mean BTD is accompanied by a decrease of the mean 10.8 µm brightness temperature and the overall trend is very similar. The highest positive BTD value occurred at 2055 UTC but the lowest brightness temperature in the 10.8 µm band for the entire life cycle of the storm on 15 and 16 August 2008 was found about 50 minutes later. However, this does not affect anything in the correlation between the BTD and 10.8 µm brightness temperature fields in every scan.

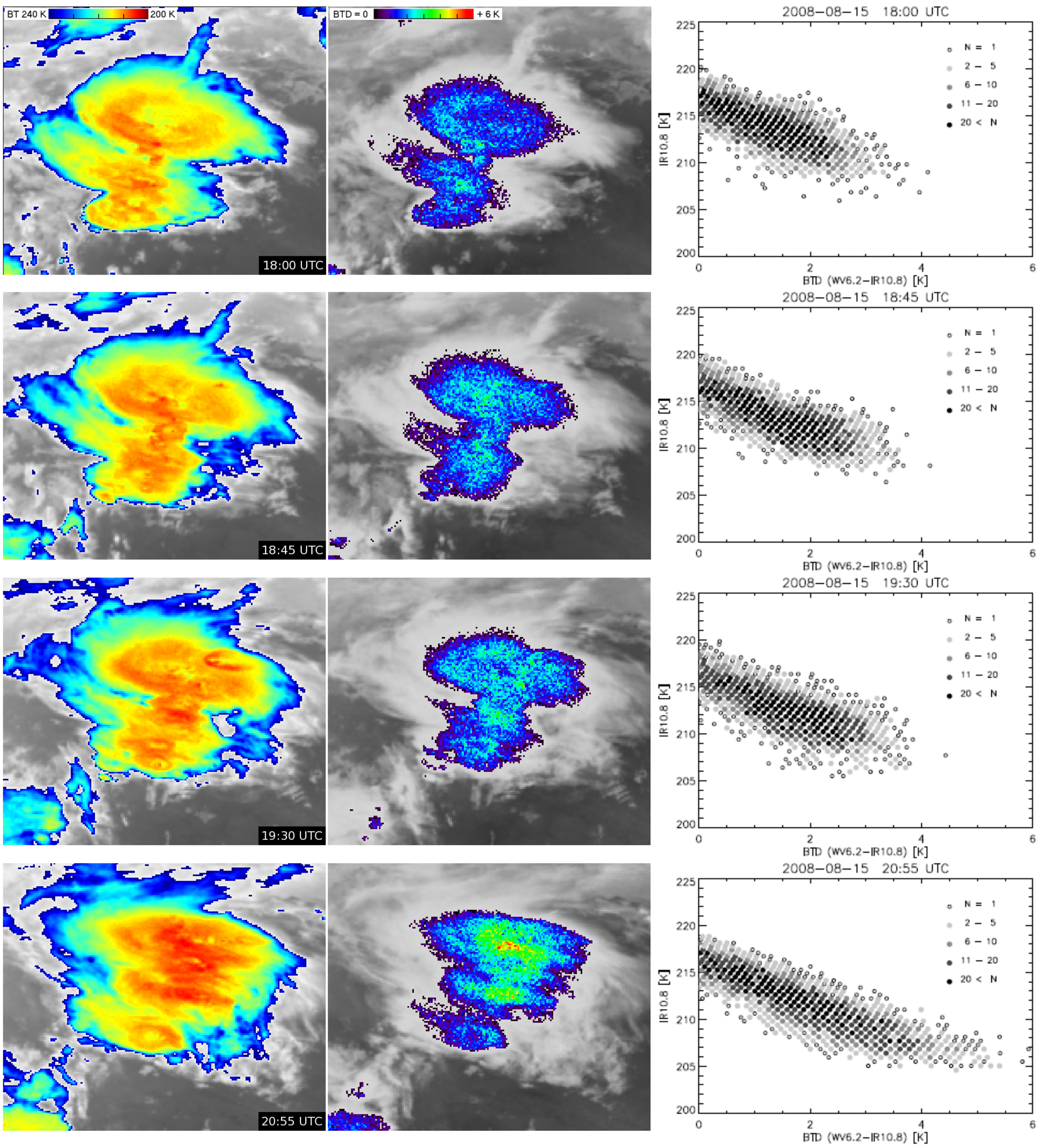

Figure 5: **The most interesting parts of the storm evolution on the 15 August 2008 above Poland and Belarus - enhanced 10.8 µm images (on the left), BTD images (in the middle) and scatterplots (on the right) of BTD (horizontal axis) and brightness temperature in 10.8 µm (vertical axis), with density distribution in grey shades – N is number of occurrences of the specific value.**

Setvák et al. (2007) noted that the highest positive BTD values may not always be found above the coldest storm tops and that the correlation between BTD and 10.8 µm brightness temperature fields could be sometimes disturbed. This discrepancy was later documented for storms on 28 June 2005 by Setvák et al. (2008). We observed the same behavior in some cases, which we refer to as “BTD anomalies”. An example of such an anomaly is the convective system on 30 May 2008 over Germany.

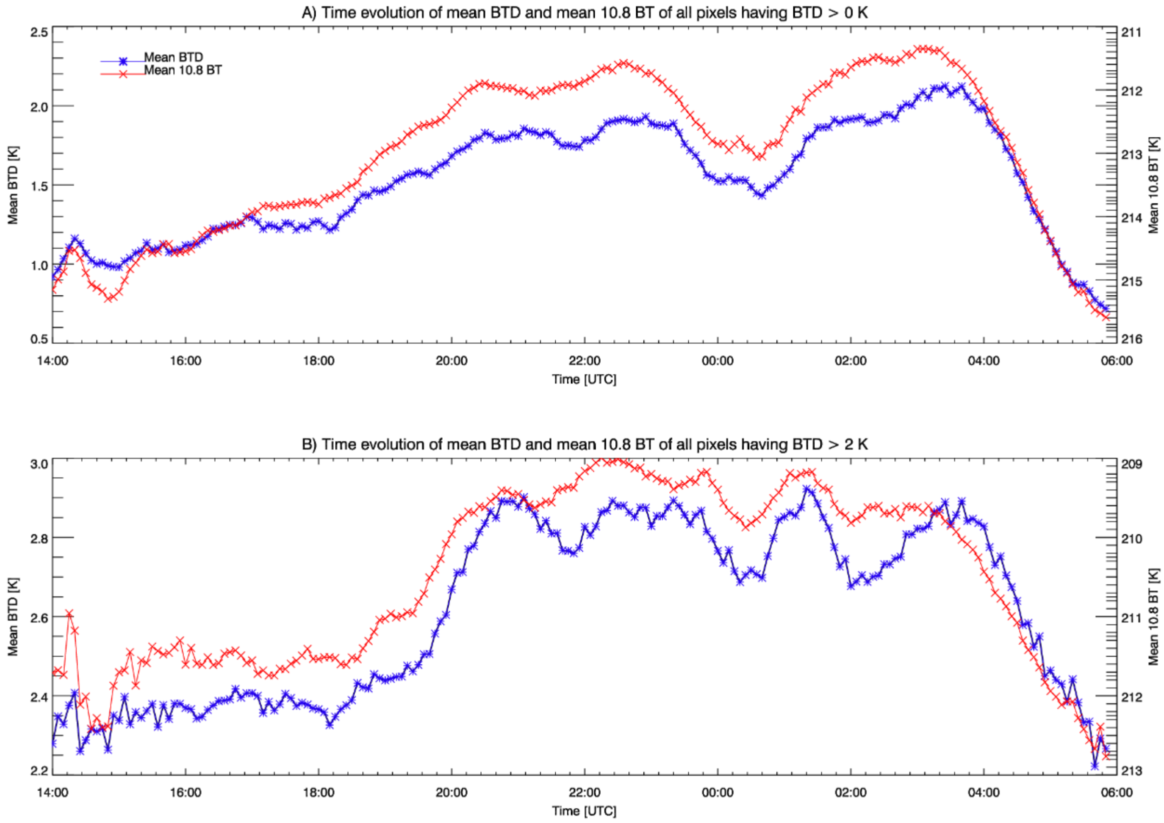

Figure 6: **Time evolution of mean BTD (blue) and mean 10.8 BT (red) of all pixels having A) BTD > 0 K and B) BTD > 2 K for the storm on 15-16 August 2008. Vertical axis for BT is opposite so the lowest values are on the top.**

The convective system occurred at about 1400 UTC and existed until 2400 UTC. The BTD anomaly developed later, at about 1730 UTC and could be observed until 2200 UTC. The appearance of the BTD anomaly and scans where the anomaly is clearly evident are shown in Fig. 7. The area of higher positive BTD is outlined in the BTD images (middle column) and the same area is also outlined in enhanced 10.8 µm images (left column) in this figure. At 1720 UTC the highest positive BTD values were still collocated with the coldest part of the storm top. However, there is no such correlation at 1730 UTC. The position of the highest positive BTD values appears to be shifted south or southwest of the coldest pixels. This continued at the next scans and persisted until about 2200 UTC. The whole system decayed one hour later. The scatterplots for this storm (Fig. 7) are also different compared to the storm on 15-16 August. Scatterplots at 1730 UTC and at later times show that some of the coldest pixels are clearly not associated with the highest BTD values. Fig. 8 depicts the time evolution of mean BTD and mean 10.8 µm brightness temperature for different subsets of the considered pixels. If we consider pixels having BTDs higher than 0 K (Fig. 8A) or 2 K (Fig. 8B), the correlation between the two mentioned functions of time is

more or less obvious. However, if we reduce the subset of considered pixels to pixels having BTD higher than 4 K (Fig. 8C) and 5 K (Fig. 8D), there is no obvious correlation between the functions. This corresponds to the observations in Fig. 7.

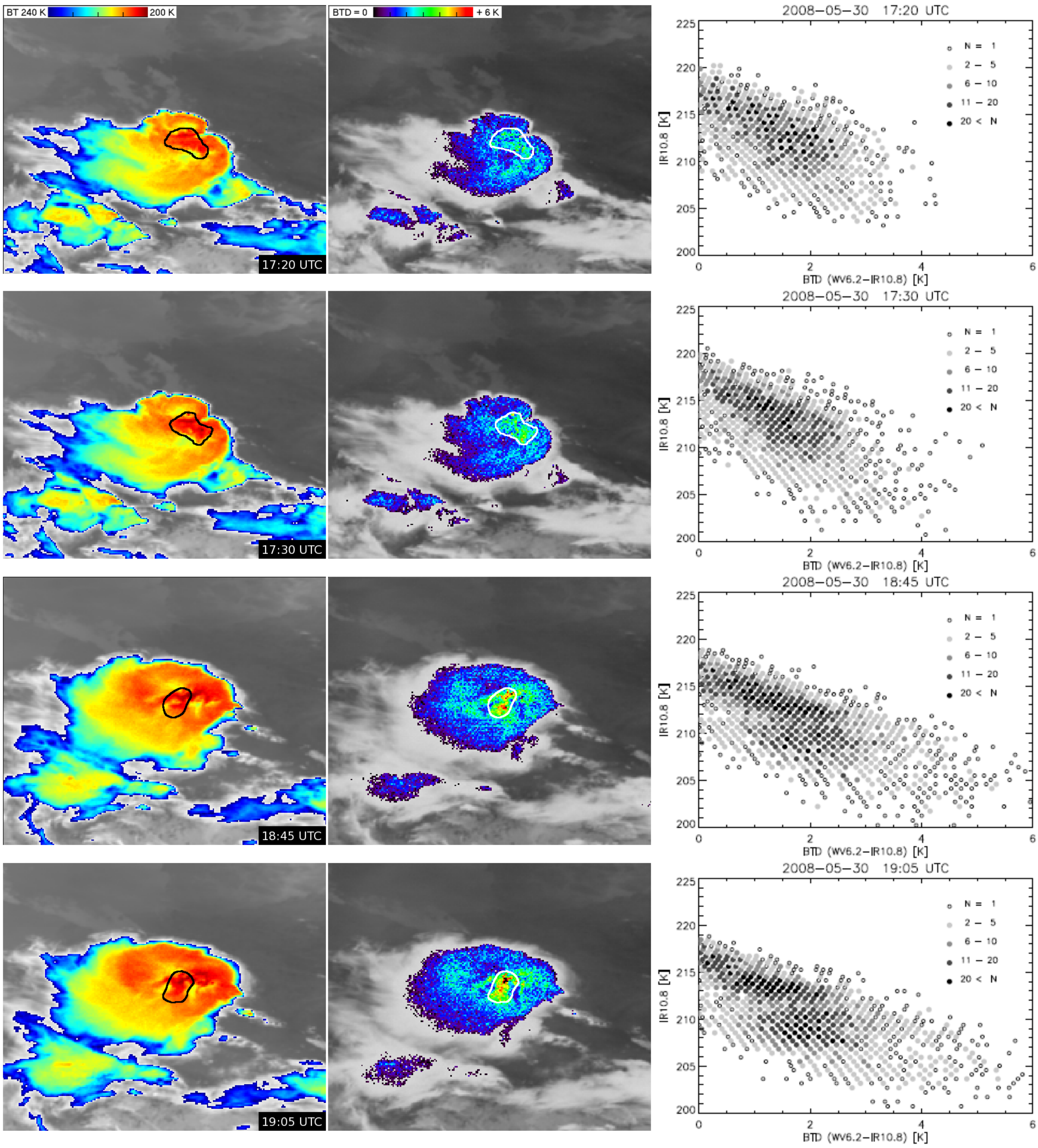

Figure 7: **The most interesting parts of the storm evolution on the 30 May 2008 above Germany - enhanced 10.8 µm images (on the left), BTD images (in the middle) and scatterplots (on the right) of BTD (horizontal axis) and brightness temperature at 10.8 µm (vertical axis) with density distribution in grey shades – N is number of occurrences of the specific value.**

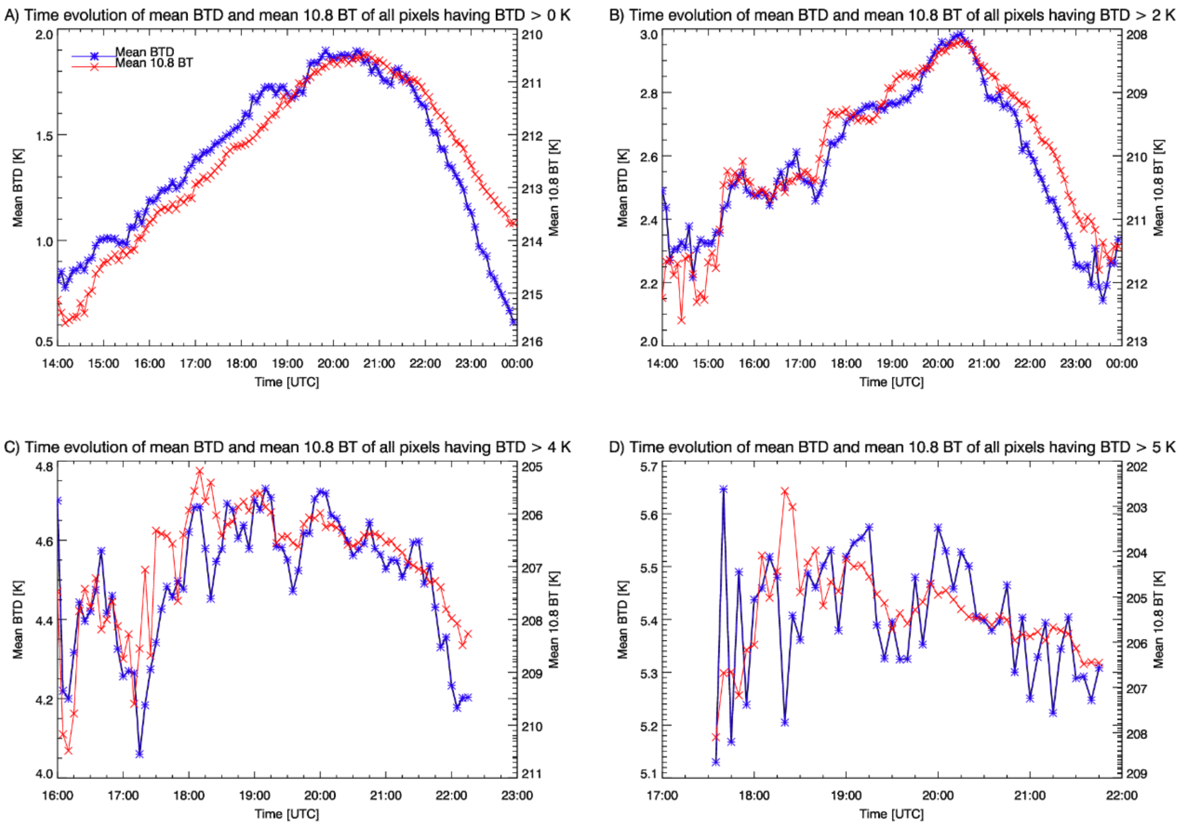

Figure 8: **Time evolution of mean BTD (blue) and mean 10.8 BT (red) of all pixels having A) BTD > 0 K, B) BTD > 2 K, C) BTD > 4 K and D) BTD > 5 K for the storm on 30 May 2008. Vertical axis for BT is opposite so the lowest values are on the top.**

CONCLUSIONS AND OUTLOOK

In this work we studied the relationship between the occurrence of positive BTD values and the stage of storm evolution and also cloud top features of convective storms using a large dataset of cases from the 2008 convective season. The majority of investigated storms show a correlation between positive BTD and 10.8 µm brightness temperature fields; however in some cases these two fields are not correlated and BTD anomalies occur. Setvák et al. (2008) offer a possible explanation that this may indicate local fluctuations of either the total amount of lower stratospheric moisture or its temperature. These fluctuations could be caused by a local moistening of the air above the storm by the storm itself, which was predicted by Pao K. Wang (e.g. Wang et al. 2009).

The dataset included some storms that exhibit cloud top features like a cold ring or cold U, but we did not observe any evident correlation between the occurrence of these and BTD fields. We have not found any case in the entire 2008 season with a BTD anomaly occurring in an earlier stage of storm evolution. This relationship between the occurrence of a BTD anomaly and maturity of convective storms corresponds to the theory that storms tend to transport larger amounts of water vapor through the tropopause, namely in their mature stage, by means of gravity wave breaking (e.g. Wang et al. 2009).

In the future, we plan to apply a similar analysis to the 2009 and 2010 convective seasons. Since the positive BTD [WV-IRW] values are alternatively attributed to storm-top microphysics, we also plan to examine the A-Train data to validate both explanations. The dataset used for this part of the study presently contains about 80 cases from Europe, South Africa, and North and South America.

ACKNOWLEDGEMENTS

Significant parts of this research were carried out under support of the Grant Agency of the Charles University in Prague – Grant No. 176210, and the Grant Agency of the Czech Republic - project 205/07/0905. The software used for satellite data visualizations was provided for research purposes by VCS. EUMETSAT/MSG data used in this study are from CHMI archive.

REFERENCES

Ackerman, S. A., (1996) Global satellite observations of negative brightness temperature differences between 11 and 6.7 micron. J. Atmos. Sci., **53**, pp 2803-2812

Brunner, J.C., Ackerman, S.A., Bachmeier, A.S., and Rabin, R.M., (2007) A Quantitative Analysis of the Enhanced-V Feature in Relation to Severe Weather. Wea. Forecasting, **22**, pp 853-872

Fritz, S., Laszlo, I. (1993) Detection of water vapor in the stratosphere over very high clouds in the tropics. J. Geophys. Res., **98** (D12), pp 22959-22967

Oltmans, S. J., H. Vömel, D. J. Hofmann, K. H. Rosenlof, and D. Kley, (2000) The increase in stratospheric water vapor from balloonborne frostpoint hygrometer measurements at Washington, D. C., and Boulder, Colorado. Geophys. Res. Lett., **27**, pp 3453-3456.

Schmetz, J., Tjemkes, S.A., Gube, M., and van de Berg, L., (1997) Monitoring deep convection and convective overshooting with METEOSAT. Adv. Space Res., **19**, pp 433-441

Setvák, M., Lindsey, D.T., Rabin, R.M., Wang, P.K., Demeterová, A., (2008a) Indication of water vapor transport into the lower stratosphere above midlatitude convective storms: Meteosat Second Generation satellite observations and radiative transfer model simulations. Atmos. Res., **89**, pp 170-180

Setvák, M., Lindsey, D.T., Novák, P., Rabin, R.M., Wang, P.K., Kerkmann, J., Radová, M., and Šťástka, J., (2008b) Cold-ring shaped storms in Central Europe. The 2008 EUMETSAT Meteorological Satellite Conference.

Wang, P.K., (2007) The thermodynamic structure atop a penetrating convective thunderstorm. Atmos. Res., **83**, pp 254-262

Wang, P.K., et al., (2009) Further evidences of deep convective vertical transport of water vapor through the tropopause, Atmos. Res. (2009), doi:10.1016/j.atmosres.2009.06.018